

THIRD EUROPEAN ROTORCRAFT AND POWERED LIFT AIRCRAFT FORUM

Paper No. 44

AN INDUSTRIAL RATIONALE FOR THE AERODYNAMIC DESIGN OF
THE FUSELAGE FOR A HIGH PERFORMANCES LIGHT HELICOPTER

M. VENEGONI, E. MAGNI, R. BALDASSARRINI

Costruzioni Aeronautiche Agusta
Cascina Costa - Varese - Italy

September 7-9, 1977

AIX-EN-PROVENCE, FRANCE

ASSOCIATION AERONAUTIQUE ET ASTRONAUTIQUE DE FRANCE

AN INDUSTRIAL RATIONALE FOR THE AERODYNAMIC DESIGN OF THE FUSELAGE FOR A HIGH PERFORMANCES LIGHT HELICOPTER

M. Venegoni, E. Magni, R. Baldassarrini

Costruzioni Aeronautiche Giovanni Agusta
Cascina Costa, Gallarate, Italy

Abstract

With the constant increase in aircraft speed a new generation of high performances helicopters has emerged. The project of such a machine certainly focuses new problems and may suggest different approaches to the rotorcraft designer.

In light of this the following paper attempts to give a general review of the industrial rationale followed in the development of the Agusta A 109 high speed helicopter. This has been done from the standpoint of the aerodynamic designer, with a particular emphasis on the problems encountered in the development of a low drag fuselage.

More recently acquired numerical methods for 3D body aerodynamic calculations have enabled us to review some aspects of the design, in view of their integration as a reliable and general working tool in the helicopter fuselages aerodynamic design.

1. INTRODUCTION

Technological and aerodynamic development has steadily improved the performances of helicopters over the years. Particularly in the class of transport helicopters the increase of commercial speed, which emphasized the potential competitiveness with fixed wing aircrafts, can be obtained increasing the engine power or the aerodynamic efficiency.

Up to the beginning of the 70's (date of definition of the A 109 final configuration) the greatest effort of aerodynamic research was placed on an increase of the rotor performances. In JAHS, AIAA, STAR index 1965-72 the 40% of the papers was devoted to the Aerodynamics of Rotary wing and of this only the 3% concerned the fuselage and non rotating components. On the other hand from figure 1, where the influence of the different portions of helicopter drag

is given versus forward speed, it is clear that the weight of the parasite drag for a typical helicopter, is predominant at high speed in the required overall power balance.

A typical break-down of the effect of the various components on the parasite drag is displayed in figure 2. The fuselage - pylon - landing gear - engine nacelles - protuberances unit usually makes the most relevant contribution to the whole. It is on this particular nucleus that most of aerodynamic optimization efforts have been concentrated in the course of Agusta's 109 aerodynamic design.

In fact technical and marketing surveys confirmed the commercial feasibility of a civil light weight helicopter while making clear that the characteristics required were to be as follows: low fuel consumption, ground mobility, comfort, in addition to a comparatively high cruising speed.

Fig.3 shows the logical development of the program. In the preliminary design stage a general layout of the helicopter is defined according to mission requirements. The remaining design process may be divided in two phases, namely minimum shape determination and its aerodynamic fairing.

In fact a helicopter may be logically broken down in two parts: an operational volume comprising the aircraft functional units, and the fairing which represents a medium between the above-mentioned operational volume and the air, so that the former may move through the latter with the least drag.

The minimum shape evaluation is carried out by means of a modular approach consisting of the design of each unit and subsequent assembly via a loop process until a satisfactory shape is achieved. It is interesting to notice that besides structural and operational criteria the design is also influenced by gross aerodynamic rules: typically frontal area minimization and volume distribution smoothing.

The fairing of the minimum shape was achieved through an evolving process of shape definition supported by a program of wind tunnel tests which aimed to obtain a final shape having not only low drag characteristics, but also a clean flow distribution in its critical parts, namely nose, pylon-hub area and lower afterbody.

Subsequent flight tests on the full size helicopter substantially confirmed the results, generally with an improvement in aerodynamics characteristics where the wind tunnel scale effect had been critical.

More recent design approaches include numerical methods as an aid to the aerodynamic analysis. A comparison with the experimental results has been carried out, showing the possibility of including these programs as a support of the design process both in the preliminary stage and in connection with the wind tunnel experimental program.

2. GENERAL LAY-OUT AND MINIMUM SHAPE EVALUATION

It is worth noting that there are aerodynamically oriented choices to be made already at this early stage. In our particular case the purpose of obtaining a fuselage as aerodynamically clean as possible suggested the inclusion of all the components inside the fuselage, so as to eliminate all protuberances. Specifically it was decided to install the engines, consisting of two independent units for reasons of reliability, inside the fuselage thus avoiding any interference effect and flow disturbance.

Similar reasons have led to the choice of a retractable landing gear. Because of the requirement of ground mobility a skid landing gear was abandoned from the beginning so that the problem was focused on the choice between a fixed or a retractable wheel undercarriage. Characteristics of easy manufacturing and maintenance of a fixed structure are offset by a not negligible aerodynamic penalty, while on the other hand a retractable system would neatly avoid the problem, even though it implies a little increase in structural weight.

An estimate of power required, together with flight tests results, obtained afterwards on the full scale helicopter, is diagrammed in figure 4 versus flight speed for the above mentioned configurations, together with the estimated A 109 operating range: one can see that the range of maximum utilization is at comparatively high speeds, where the payoff of the retractable landing gear is considerable.

The helicopter was subsequently broken down into the modules listed in figure 5. Their final assembly is presented in figure 6. Each one had been defined through its appropriate operational requirements (for example mobility and comfort for the passenger compartment, efficient safe and comfortable airscrew operation for the cockpit, and so on) consistently with the structural design.

3. AERODYNAMIC DESIGN

The program was carried out, with the support of wind tunnel tests on reduced scale models with simulated rotor downwash, the test section was of the open type and measurements were made with a 6 components internal balance (figure 8).

The problems involved in the reduced scale testing procedure were well known, particularly regarding the Reynolds number simulation with the consequent differences in the behavior of the boundary layer between the model and the full scale fuselage. Nevertheless it was felt that, with an unavoidable degree of uncertainty implied by reduced scale tests, a significant

set of results could be obtained, both quantitative and qualitative, which could be extrapolated to the full size fuselage.

A preliminary analysis of the minimum shape revealed the following: limited possibilities of intervention existed for central fuselage fairing, whereas the nose and even more the aft portion afforded greater flexibility. This led to the development of a program of evolutive shape definition in which the central body remained unchanged.

In fact a geometrical survey of the minimum shape shows that for the purpose of frontal area minimization the central part must be enveloped as closely as possible by the fairing: this was achieved with a fairing surface having a quasi-rectangular cross section with rounded corners not comprising the pylon, the latter being developed independently.

As for the forebody fairing, the analysis of figure 6 shows that it is less subject to geometrical constraints. The wind tunnel tests on the first nose shape emphasized its extreme importance as a conveyor of the flow towards the central body, especially onto the pylon. It is for this reason that its design was modified later on, in order to reach a more satisfactory shaping of the streamlines flowing rearwards.

Finally, the tail was subject only to the following constraints: that the anti-torque rotor may have its design distance from the mast and ground clearance, and that its transmission system be externally located for easy inspection.

The first model (figure 7) obeyed the classical concept of the helicopter, where the tail is not so much an aerodynamically integrated part of the rest of the fuselage, but rather a structural appendix supporting the empennages and the tail rotor (Model A). The tail has no useful aerodynamic role and the flow coming from the central body bulk separates, possibly because of the strong local sectional area contraction, as flow visualizations show.

It became clear as well as that the helicopter drag would drop dramatically if the air flow could be forced to contract much more before separation, so that the wake could be accordingly thinned. This was sought through a smoother variation of the sectional area, in order to induce the flow to follow the afterbody contour while at the same time keeping the tail volume as low as possible, so as minimize its wetted area.

Unfortunately, as figure 11 shows, model B wasn't capable of any drag reduction in comparison with model A. Flow visualizations show in fact areas of flow separation and large scale turbulence on the lower surface, which are provoked by an excessive pressure recovery. It must be taken into consideration that the rotor wake at the flight speeds simulated in the test impinges on the tail, giving among other effects an unwanted downward slant to the flow. For this reason the most critical part

of the tail is the lower portion, and efforts have been concentrated on it to improve its aerodynamical behaviour.

In model C the lower afterbody was different and even more smoothly blended with the central body bulk, so that a total merging with it was reached. Experimental data justified this trend yielding a reduction in drag coefficient for model C, but mainly a very good flow distribution in the afterbody area.

Another important problem dealt with was the airflow behaviour in the rotor hub area. Here the pylon plays an important role: its design objectives have been not only local additional drag minimization, but also an appropriate shaping of the flow, in view of reducing its interaction with the hub to a minimum.

In figure 12 the types of fairings tested are presented. In the early models different surfaces were superimposed on the pylon for the purpose of keeping the flow parallel to the central body upper surface; however the tests showed that this was also feasible by simply modifying the shape of the pylon itself. As figure 12 shows pylon 5 is the best from the drag reduction viewpoint. Visualizations confirm this, showing an exceptionally adherent flow around the pylon and over the fuselage. The model has a comparatively thin NACA family section with a penetrating front portion, which obtains the maximum adherence of the flow otherwise tending to separate from the lateral surface.

Figure 9 gives an evidence of the nose-nylon aerodynamic interaction. From this point of view the best condition around the midbody is achieved when the flow at the helicopter neutral attitude (i.e. zero pitching and yawing angles) follows the body's waterlines. This happens when the asymptotic flow is parted preferably along the horizontal plane, rather than the vertical, in order to avoid that an excessive mass of air be bent upwards towards the rotor.

It is worth remembering that the slope of the windscreen is limited by pilot visibility requirements and at all events the radius between the roof and the windscreen must be sufficiently large, in accordance with the constraints imposed by the cockpit, in order to forestall phenomena of separation and vortices formation which could considerably disturb the downstream flow. Figure 10 shows the progressive development of the helicopter forebody: by increasing the radius of curvature on the lateral portion of the nose and windscreen in the horizontal and vertical plane, and decreasing it along the symmetrical plane, the desired goals of flow shaping were reached. This was achieved without penalties in any of the aerodynamic characteristics of the entire model. As at the high design flight speed of the helicopter the deflected rotor wake interacts with the fuselage only in its rear portion (so that the fuselage behaves as a body immersed in great part inside an asymptotic flow), it was felt

that the airflow behaviour observed on the model would be substantially the same in reality, i.e. the interaction between the air flowing over the fuselage and that concerning the rotor would be kept to a minimum. Flight tests visualizations carried out with prototypes have confirmed the validity of these statements.

4. COMPARISONS

It was from the flight tests that we tried to have a confirmation of the hypotheses adopted in the development of the program. Moreover the evolution in the mid 70's of numerical methods capable of simulating the three-dimensional aerodynamic behaviour of fuselages, enabled us to use these methods as an a-posteriori verification, proving the validity of their use in the design process.

4.1 Flight Tests

Tests were run on prototypes both for a quantitative survey of the helicopter behaviour, and for a number of qualitative verifications of the reduced scale tests results.

Photographic records (still and cine) were taken of a helicopter with a wool thread set up. The pictures show the excellent agreement with the aerodynamic field observed on the small scale models (figures 13 to 18). It can be noticed that at high speed, where the fuselage attitude is very close to neutral with zero yaw and pitch angles, the effect of the nose is the one looked for: the oncoming flow is conveyed for its greatest part along the central body waterlines.

Very good flow adherence is also found in the pylon area (which is affected from the hub wake only in the aft region). Moreover there is a most satisfactory behaviour of the flow in the most critical portion of the fuselage, that is the lower junction between the mid-body and the tail: the visualizations always show a smooth distribution of velocities and a constant adherence of the airstream (as shown in figure 15 for a maneuver condition).

4.2 Numerical Methods

The experimental program has emphasized the need for a theoretical tool to employ in the aerodynamic design and verification of three dimensional bodies.

Two important items have emerged:

1. Much more can be understood from the experimental data if the physical phenomena can be theoretically interpreted.

2. Design time and cost can be greatly reduced if shape modifications, and in general any change in the tested configuration, can be verified in real time.

As a logical consequence a computer program has been set up for the three dimensional analysis of bodies in viscous flow. The program consists of two sections: in the first a potential flow analysis is carried out. Its outputs are employed by the second part for the streamlines and boundary layer calculation. Through an iterative process between the two blocks it is possible to obtain an approximate solution of the problem.

The whole process of aerodynamic design of the A 109 has been reviewed with the aid of the newly developed analytical method: thus it has been possible to check some of the assumptions made in the course of the testing program, and at the same time to ascertain the limitations of the numerical method itself. These may be summarized as follows:

1. The inability, common to all existing mathematical models in the authors' knowledge, of the program to satisfactorily calculate separated flows and wake regions.
2. The restriction concerning the lift characteristics mathematical representation on irregular bodies, as fuselages generally are.

On the other hand however the program yields a series of results which, if suitably exploited, may give useful information to the helicopter designer, not only in the aerodynamic field, but also in the structural, for the analysis and/or verification of aerodynamically stressed fuselage components. Some examples of the program's outputs (velocity vectorial distribution, surface streamlines, pressure coefficient trends along the fuselage upper and lower surfaces) are given in figures 19 to 23.

These results, as above mentioned showed an excellent agreement with the visualizations observed both on the small scale models in the wind tunnel facility, and on the full scale helicopter in the course of the flight tests, and confirmed the clean design of the final model.

Concluding Remarks

The design approach followed in the definition of the nose and pylon shapes has allowed to give the air flowing around the fuselage a preferential orientation in the horizontal plane, thus avoiding an excessive upward deflection of the stream which might have interacted negatively with the rotor.

Considerable emphasis was given in the design of the lower afterbody portion which is critical from the standpoint of flow

separation. The final configuration reached this goal, showing also that the relatively large volume of the tail boom has not given deleterious force and moments generated by rotor downwash.

It has been confirmed that a reliable 3D potential flow numerical method is particularly useful in the preliminary definition and during the design of a helicopter of the class above considered as a support of a wind tunnel program.

The flight tests results have confirmed the employability of small scale wind tunnel facilities and numerical support in an industrial rationale for the design of a light weight high speed helicopter.

The future development of rotorcraft design will include numerical programs in growing measure, and along this line much more sophistication will be required for the modeling of the totality of the aerodynamic field, including the rotors wakes interaction, and a more satisfactory definition of 3D viscous phenomena on bodies, typically transition and separation effects.

REFERENCES

1. A. Gessow and G.C. Myers Jr., Aerodynamics of the helicopter, Frederick Ungar Publishing Co. New York
2. Sighard F. Hoerner, Fluid dynamic drag, published by the Author, Midland Park New Jersey 1965
3. A. Pope and J.J. Harper, Low speed Wind Tunnel testing, John Wiley & Sons Inc., New York - London - Sydney 1966
4. R.C. Dingeldein, Considerations of methods of improving helicopter efficiency, NASA TN D-734, April 1961
5. J.C. Biggers, J.L. McCloud III and P. Patterakis, Wind Tunnel tests of two full-scale helicopter fuselages, NASA TN D-1548, October 1962
6. W.Z. Stepniewski, Basic aerodynamics and performance of the helicopter, AGARD LS-63, March 1973
7. P. Fabre, Problèmes de trainée des appareils a voilures tournantes, AGARD LS-63, March 1973
8. S.N. Wagner, Problems of estimating the drag of a helicopter, AGARD CP-124, October 1973
9. C.N. Keys and R. Wiesner, Guidelines for reducing helicopter parasite drag, Journal of the American Helicopter Society, January 1975

10. R.M. Williams and P.S. Montana, A comprehensive plan for helicopter drag reduction, Proceedings of the National Symposium on Helicopter Aerodynamic Efficiency, American Helicopter Society, March 6-7 1975
11. J.P. Rabbott and R.H. Stroub, Wasted fuel - Another reason for drag reduction, Proceedings of the National Symposium on Helicopter Aerodynamic Efficiency, American Helicopter Society, March 6-7 1975
12. A.F. Smith, Effects of parasite drag on rotor performance and dynamic response, Proceedings of the National Symposium on Helicopter Aerodynamic Efficiency, American Helicopter Society, March 6-7 1975
13. J.M. Duhon, Cost benefit evaluation of helicopter parasite drag reduction, Proceedings of the National Symposium on Helicopter Aerodynamic Efficiency, American Helicopter Society, March 6-7 1975
14. A.M. Bosco, Aerodynamic of helicopter components other than rotors, AGARD CPP-111, September 1972
15. P.E. Rubbert et al, A general method for determining the aerodynamic characteristics of fan-in-wing configurations, NTIS 667 980, December 1967
16. J.L. Hess and A.M.O. Smith, Calculation of potential flow about arbitrary bodies, Progress in Aeronautical Sciences, Vol.8, Pergamon Press, 1967
17. F.O. Smentana, D.C. Summey, N.S. Smith and R.K. Carden, Light aircraft lift, drag and moment prediction - A review and analysis, NASA CR-2523, May 1975

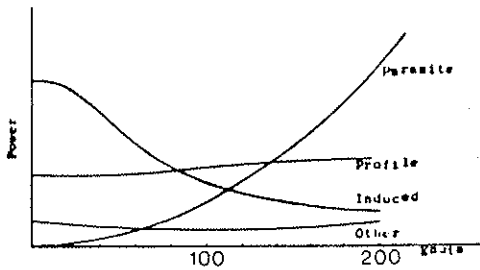


Fig.1 Typical breakdown of helicopter power losses

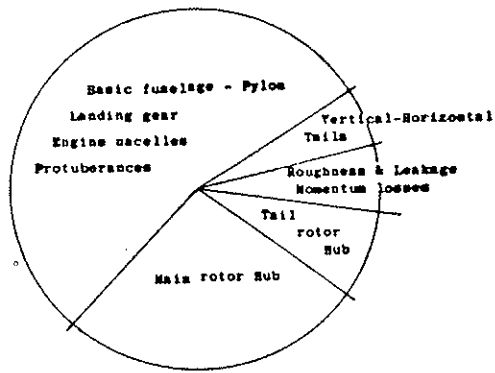


Fig.2 Typical parasite drag breakdown

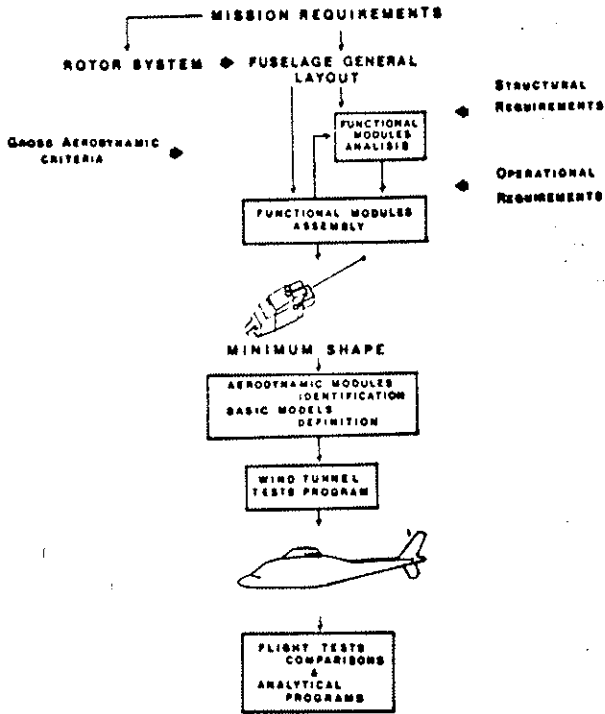


Fig 3 Development of the Program

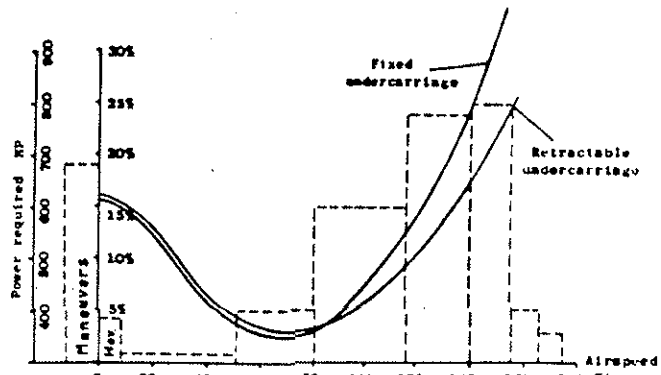


Fig.4 Comparison of total required power for an helicopter with fixed and retractable undercarriage & Employment Spectrum

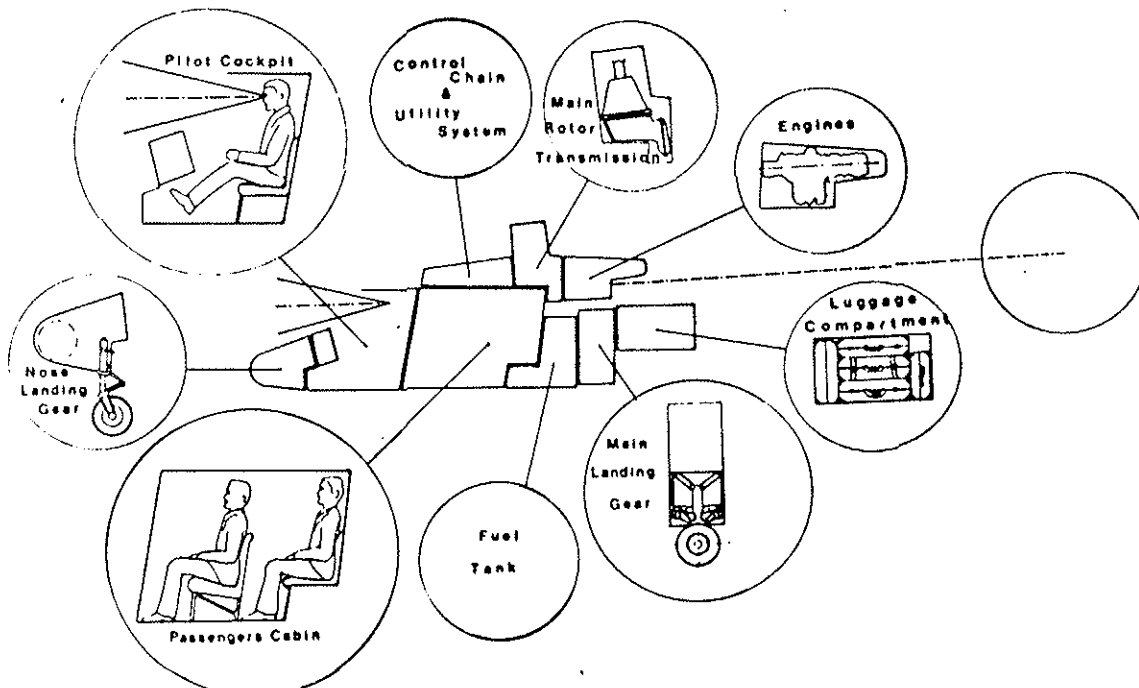


Fig 5 Final Modules assembly

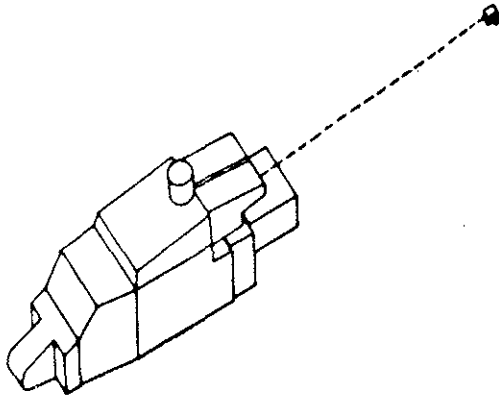


Fig 6 "Minimum Shape"

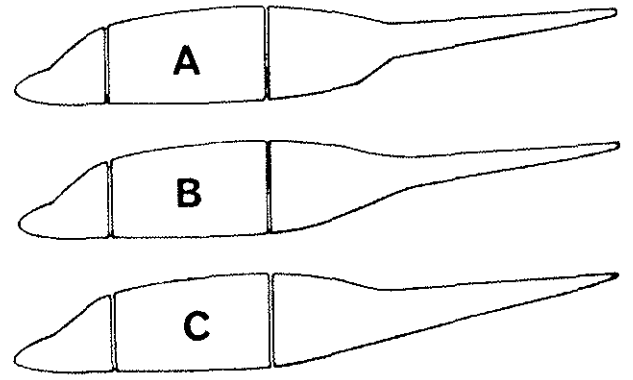


Fig.7 Wind tunnel models evolution



Fig.8 Model Installation in Wind Tunnel

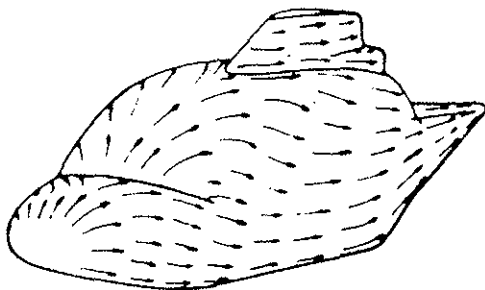


Fig 9 Flow Visualization around Model C

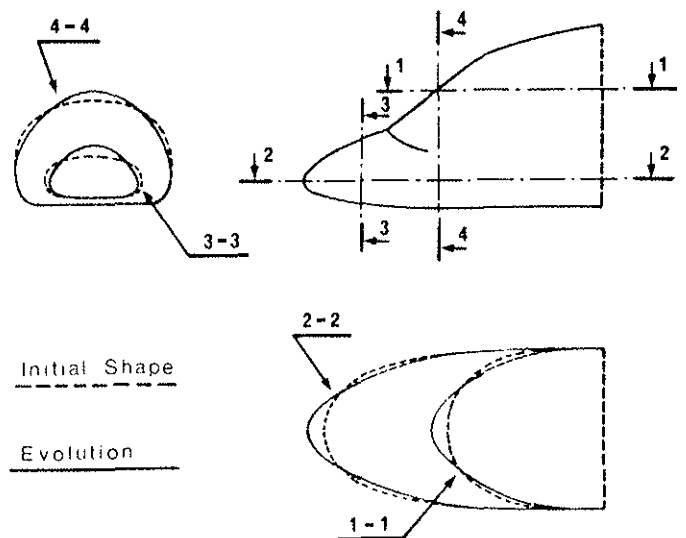


Fig.10 Nose shape evolution

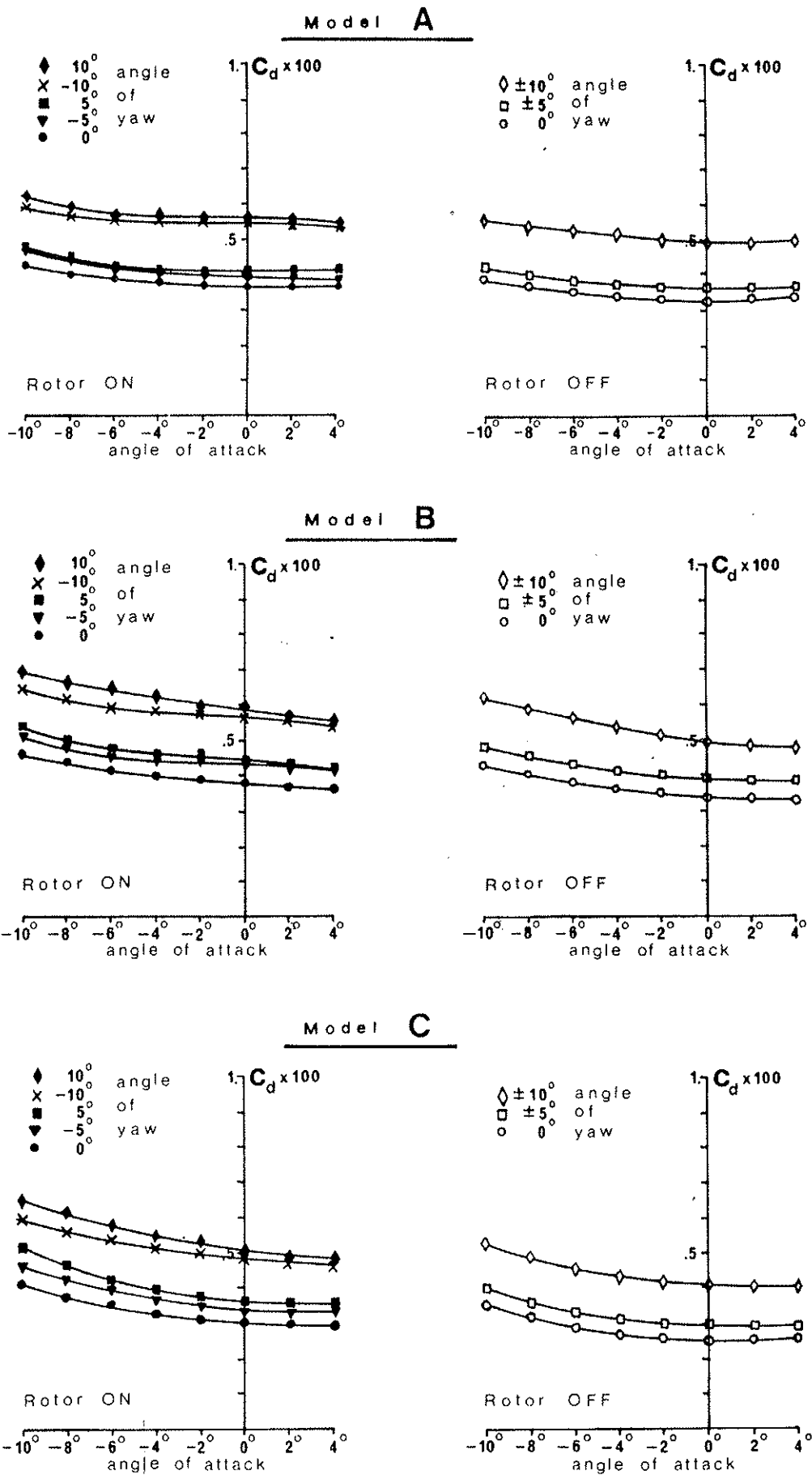


Fig 11 Drag characteristics of the three Models

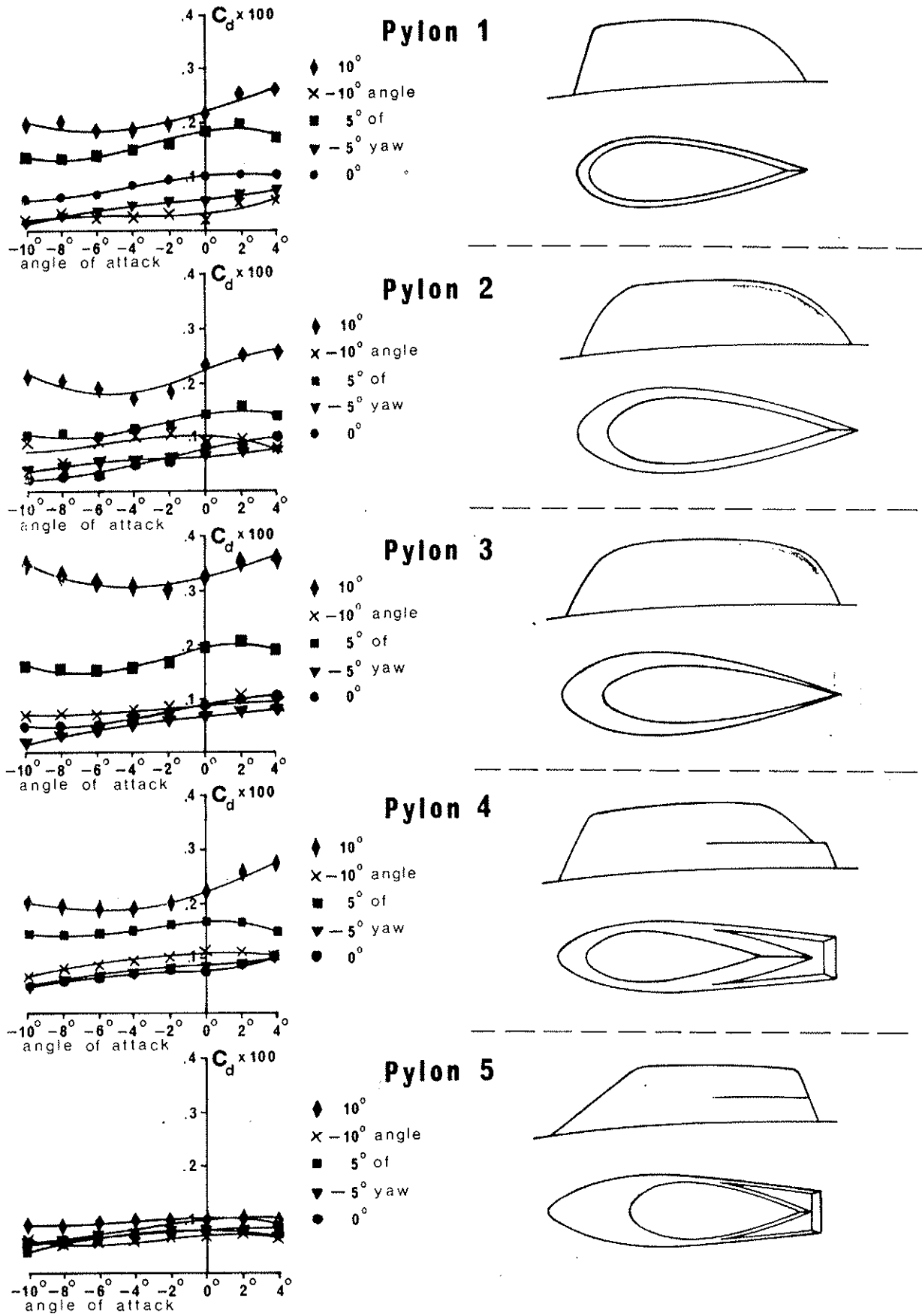


Fig 12 Comparison of incremental drag for different pylons

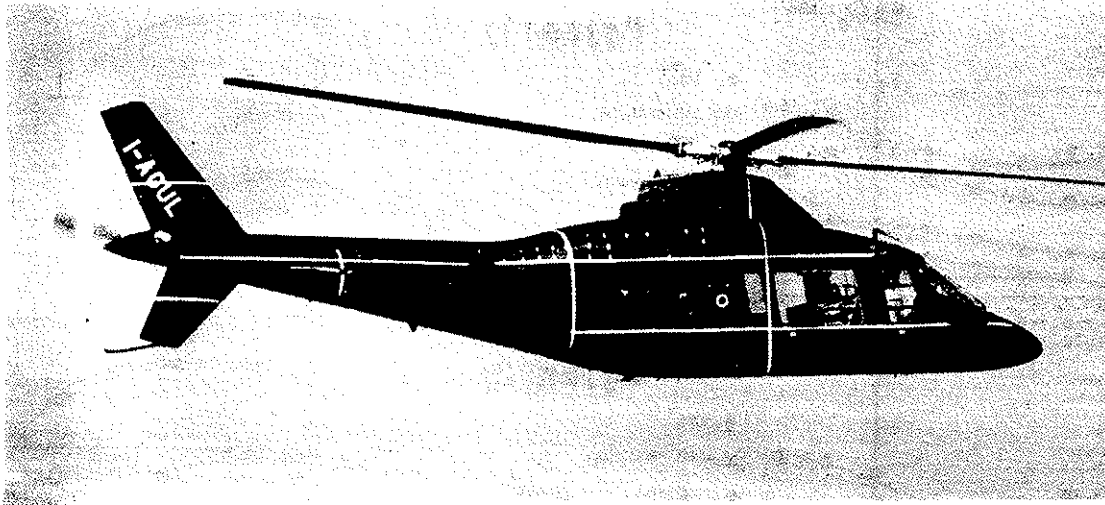


Fig.13 A 109 Wool Thread Visualization - 140 Knots

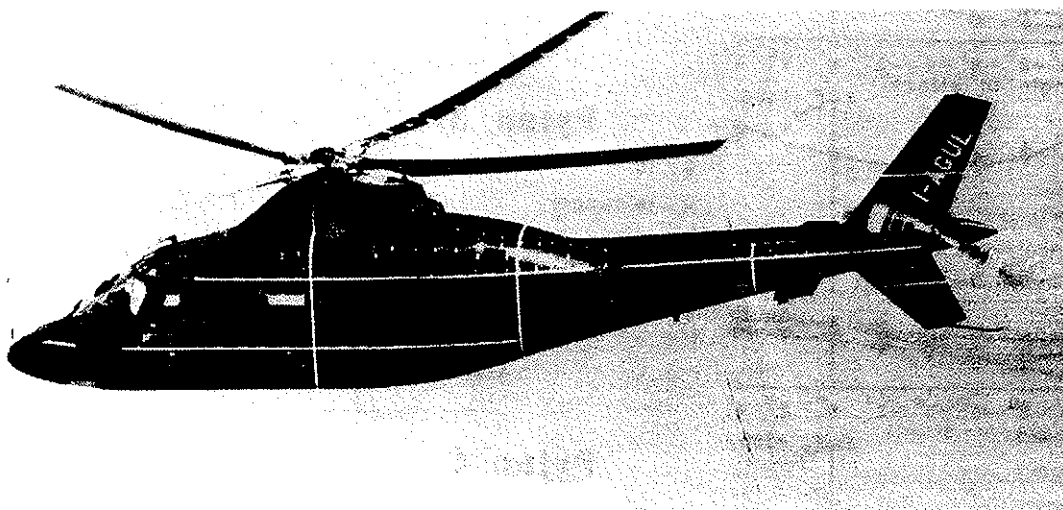


Fig.14 A 109 Wool Thread Visualization - 140 Knots

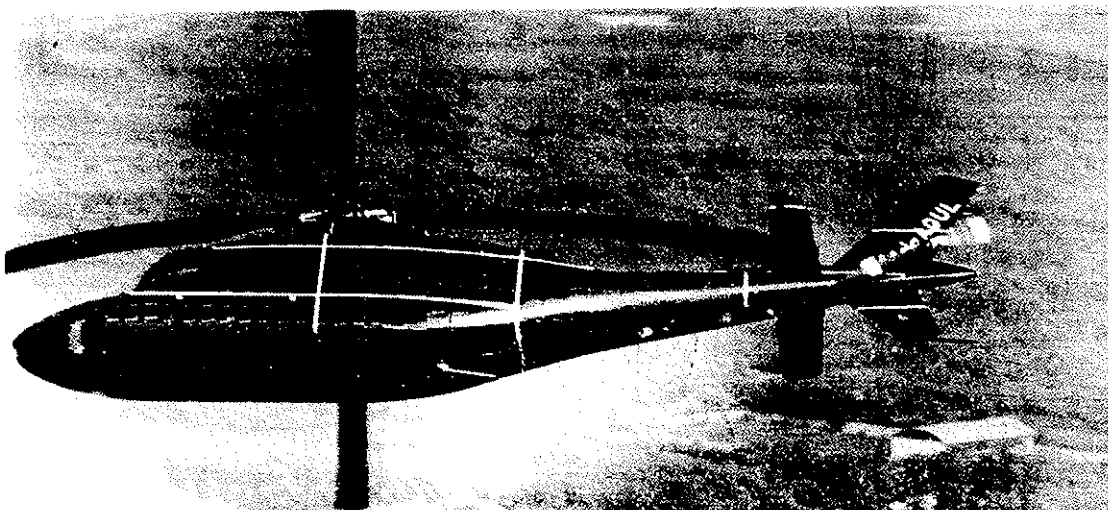


Fig.15 A 109 Wool Thread Visualization - Turn

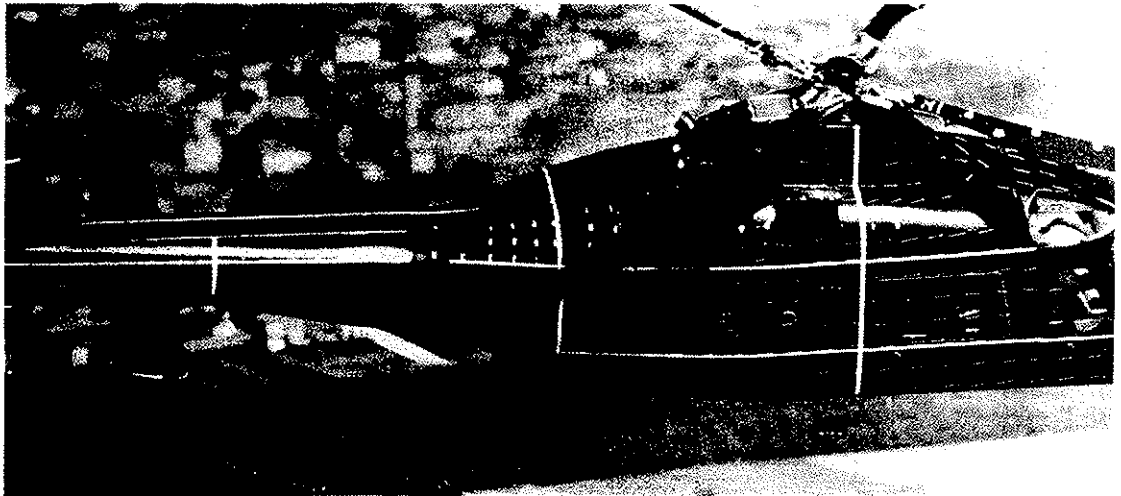


Fig.16 A 109 Wool Thread Visualization - 140 Knots

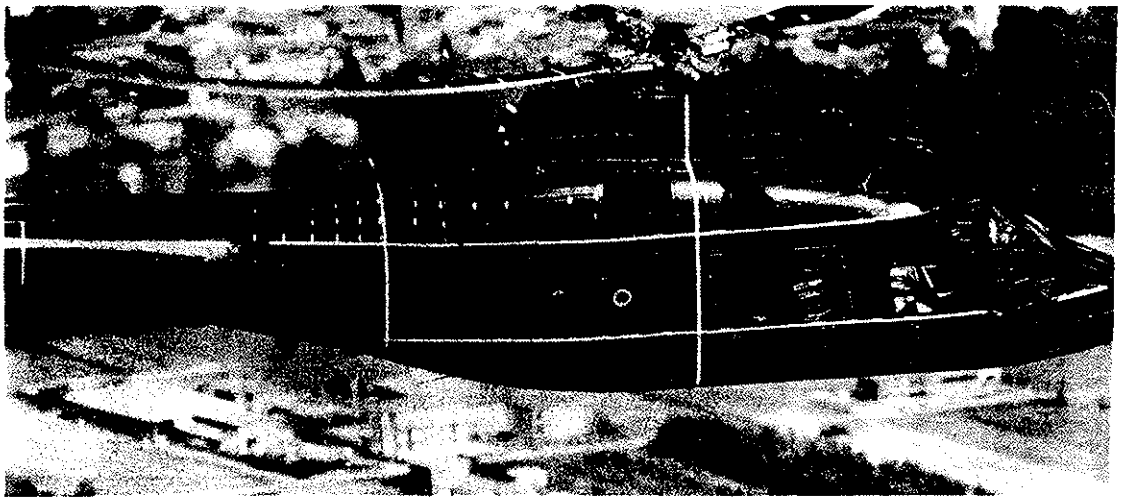


Fig.17 A 109 Wool Thread Visualization - 120 Knots

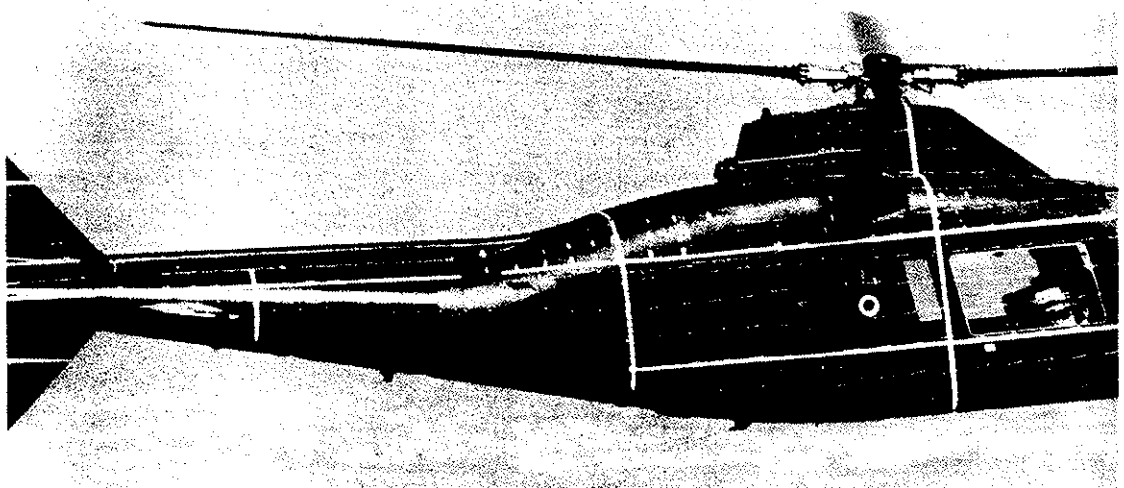


Fig.18 A 109 Wool Thread Visualization - 80 Knots

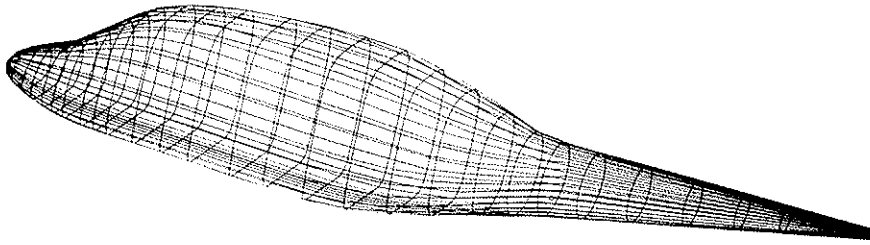


Fig. 19 Sample Input for Numerical Program

Model C Schematization

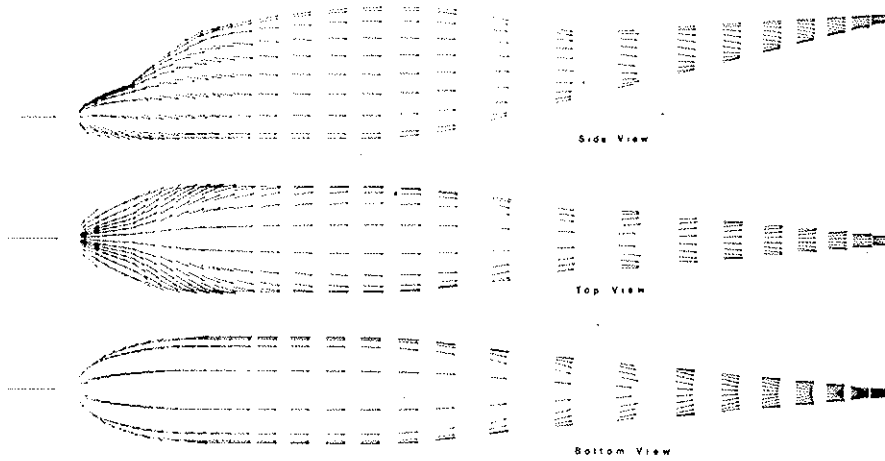


Fig. 20 Surface Velocity Distribution on Model C

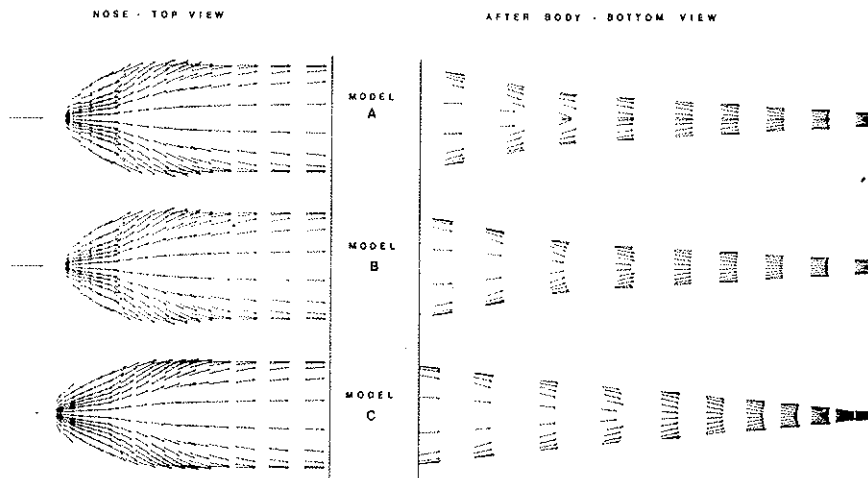


Fig. 21 Comparison of Flow Velocity Distribution on the Three Models

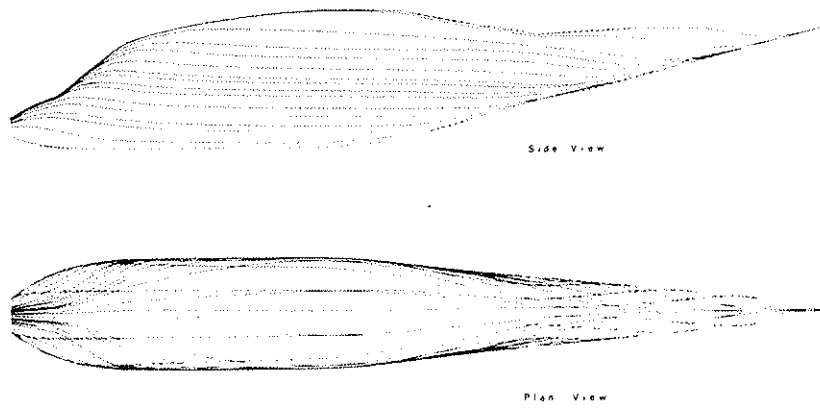


Fig. 22 Streamlines Distribution over Model C

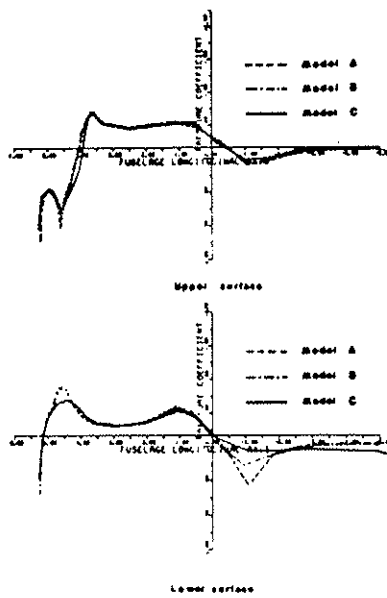


Fig. 23 Pressure distribution along the models

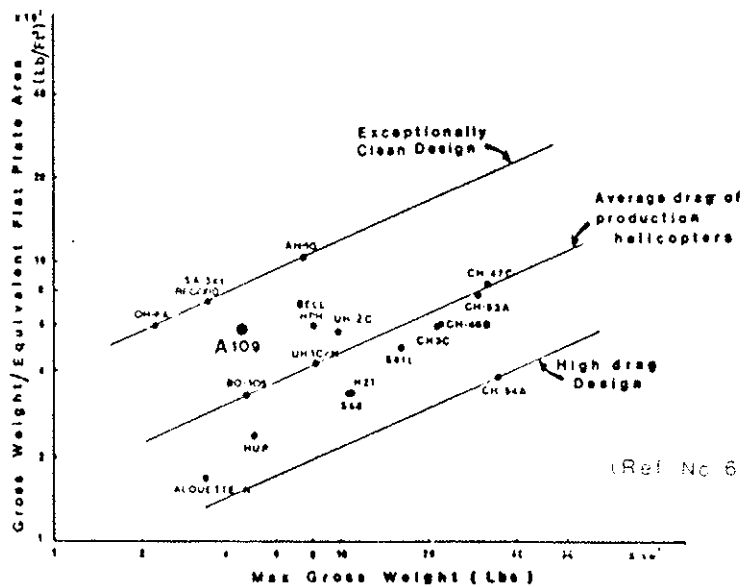


Fig. 24 Equivalent Flat Plate Area vs Maximum Gross Weight